Received: 22 September 2023 | Revised: 8 January 2024 | Accepted: 27 January 2024

DOI: 10.1002/jbm.b.35390

RESEARCH ARTICLE

Society For Biomaterials | WILEY

Functionalization of a zirconia surface by covalently immobilized fibronectin and its effects on resistance to thermal, acid, and mechanical exposure

Alena L. Palkowitz[1] | Taskin Tuna[2] | Robert Kaufmann[3] | Eva Miriam Buhl[4] | Stefan Wolfart[2] | Horst Fischer[1]

[1]Department of Dental Materials and Biomaterials Research, RWTH Aachen University Hospital, Aachen, Germany

[2]Department of Prosthodontics and Biomaterials, RWTH Aachen University Hospital, Aachen, Germany

[3]DWI Leibniz-Institute for Interactive Materials, RWTH Aachen University, Aachen, Germany

[4]Electron Microscopy Facility, Institute of Pathology, RWTH Aachen University Hospital, Aachen, Germany

Correspondence
Alena L. Palkowitz and Horst Fischer, Department of Dental Materials and Biomaterials Research, RWTH Aachen University Hospital, Pauwelsstrasse 30, 52074 Aachen, Germany.
Email: alena.palkowitz@rwth-aachen.de and hfischer@ukaachen.de

Funding information
German Research Foundation, Grant/Award Numbers: 495328185, WO 1576/6-2, FI 975/30-2

Abstract

Silane chemistry has emerged as a powerful tool for surface modification, offering a versatile means to enhance the properties of various substrates, such as dental implant abutment materials. In this study, we investigated the stability of the 3-aminopropyldiisopropylethoxysilane (APDS) layer on yttria-partially stabilized zirconia (Y-TZP) surfaces after mechanical, acid, and thermal treatment in order to simulate fluctuations within the oral cavity. To accomplish that, the viability of human gingival fibroblasts on APDS-modified surfaces after applied treatment strategies was assessed by live/dead staining. Moreover, the hydrolysis stability and enzymatic degradation resistance of crosslinked fibronectin to the APDS layer was examined by immunostaining and western blot. The results revealed that the applied modifications were not affected by the different treatment conditions and could withstand the fluctuations in the oral cavity. Furthermore, crosslinked fibronectin on silanized Y-TZP was stable against hydrolysis over 21 days and enzymatic degradation. We thus can conclude that the proposed functionalization method has high potential to tolerate harmful effects within the oral cavity and remains unchanged on the surface.

KEYWORDS
acid resistance, mechanical stability, SAMs, thermal stability, zirconia

1 | INTRODUCTION

The oral cavity with its natural teeth, as well as dental and implant prosthetic restorations, is constantly exposed to different pH values, temperatures, and mechanical stresses. Temperature and pH fluctuations, oxygen, bacteria, and the decomposition of food constantly attack its surfaces and interfaces.[1] The physiological pH range for resting saliva is between 6.2 and 7.6.[2] When the pH of saliva is decreased up to <5.5 during eating or drinking, a critical pH is reached that could result in dissolution of the mineral of the enamel.[3] A constantly forming thin layer called acquired pellicle protects the surfaces in the oral cavity, especially the teeth, from various influences such as mechanical abrasion and direct contact with acids, thus providing a natural barrier.[4] The pellicle is an acellular protein film derived from saliva, which has a strong adhesion to the enamel and is difficult to remove by brushing. It has also been found on surfaces of dental fillings and reaches a depth of 10–20 nm within 1 min.[5–7] In detail, the pellicle reveals a knotted, globular surface texture and consists of absorbed protein aggregates and other macromolecules from the oral environment such as salivary glycoproteins, phosphoproteins, lipids,

and immunoglobulins.[8,9] Only specific proteins within the saliva are found in the initial enamel cuticle, including statherine, histatin, and proline-rich proteins.[10,11] Because of the semipermeable character of its membrane, the pellicle protects the tooth surface from excessive losses of calcium and phosphate and thus from acid influences.[5,12] Since all surfaces are covered by the pellicle in the oral cavity, abutment surfaces are also affected.

High performance oxide ceramics, such as zirconia and especially yttria-stabilized zirconia (Y-TZP), are frequently used as dental abutment material.[13] Its low Young's modulus, low thermal conductivity, high biocompatibility, and white color have made Y-TZP an attractive alternative to titanium, the gold standard, for dental abutments.[14–18] However, because of the bioinert character of Y-TZP, rapid bonding with soft tissue is limited. For this reason, it is enormously important to choose surface functionalization strategies that can facilitate cell adhesion in order to overcome cell bonding limitations.

The application of self-assembled monolayers (SAMs) is a well-established technique to chemically activate surfaces.[19] SAMs are nanometer-thick monolayers made of molecules that can covalently bind to the substrate material and, due to the intermolecular interactions, can form a closed layer with a locally highly ordered structure. The molecules are characterized by three functional sections: (i) a head group, which forms a covalent bond with the substrate material, (ii) an organic backbone, and (iii) a terminal group, which determines the surface properties and thus its interaction with the surface environment.[20,21] Different functional groups such as —OH, —CH_3, —COOH, and —NH_2 can be used to control hydrophobicity or to induce bioactivity.[21–23] In this way, SAMs can be used to connect proteins from the extracellular matrix (ECM) to the material's surface.[24] Fibronectin (FN) in particular is a ubiquitous ECM glycoprotein that plays an important role in many biological processes such as cell adhesion, migration, and differentiation.[25] Moreover, FN contains various amino acid motifs such as arginine-glycine-aspartic acid (RGD) that can be recognized and bound by the cells' transmembrane integrins.[25] Because of the predominantly aqueous and enzyme-rich environment in vivo, different crosslinkers were used for stable interconnection of the ECM protein to the silanized surface.[26] The application of additional coupling agents such as bis(sulfosuccinimidyl)suberate (BS^3) can enable a nucleophilic reaction with the amines present on the organosilane molecule, thus ensuring stable immobilization of the biomolecules.[27]

In this study, the hypothesis tested was whether the modification construct on Y-TZP surfaces would withstand mechanical, thermal, and acid exposure. To accomplish this, the stability of the 3-aminopropyldiisopropylethoxysilane (APDS)-modified zirconia specimens was assessed by scanning electron microscopy (SEM), atomic force microscopy (AFM), and X-ray photoelectron spectroscopy (XPS) after these applied different treatment strategies. The remaining APDS on the samples before and after treatment was verified via ninhydrin assay. Because it is known that the pellicle acts as a protective membrane against external stimuli on the tooth surface, the specimens were additionally covered with saliva. Because of the formation of the APDS layer on the specimen surface, the stable immobilization of fibronectin against hydrolysis and proteolytic digestion was tested using immunostaining and western blot. Finally, the cell viability on the surface after mechanical, acid, and temperature treatment was evaluated by live/dead staining.

2 | MATERIALS AND METHODS

2.1 | Zirconia sample preparation

Yttria partially stabilized zirconia (TZ-3YSB-E powder, Tosoh, Japan) specimens were manufactured by uniaxial dry pressing using a stainless steel cylindrical mold with a diameter of 9 mm and a thickness of 1.5 mm. Subsequently, Y-TZP discs were sintered at 1500°C for 2 h in a ceramic furnace (Therm-Aix, Aachen, Germany). Afterwards, the specimens were ground using 40 and 74 µm discs and polished using diamond pastes (15 and 9 µm, ATM, Mammelzen, Germany). This procedure resulted in a roughness value of R_a < 0.2 µm. Then, ceramic discs were heated to 450°C for 15 min in order to remove organic residues. Finally, the discs were cleaned by sonication in 70% ethanol (Schmittmann, Düsseldorf, Germany) and Milli-Q water (Sartorius, Göttingen, Germany).

2.2 | Silanization of the samples

To generate a silane monolayer on the surface of the discs, the specimens were hydroxylated in a solution of sulfuric acid (Sigma Aldrich, USA) and 30% hydrogen peroxide (Merck, Darmstadt, Germany) for 1 min (dilution ratio 3:1) and rinsed thoroughly in Milli-Q water (Sartorius, Göttingen, Germany). After drying at room temperature, Y-TZP discs in a round bottom flask were dipped in a 5-vol % APDS solution (Gelest, Morrisville, USA) mixed with anhydrous toluene (Sigma Aldrich, St. Louis, USA) for 3 h at 120°C under reflux. Afterwards, samples were thoroughly cleaned by 3-min wash steps with toluene (VWR, Radnor, USA) and Milli-Q water (Sartorius, Göttingen Germany) in order to remove unbound molecules. The specimens were dried overnight at room temperature.

2.3 | Crosslinking of ECM proteins to silanized samples

Coupling of the ECM protein fibronectin (Merck, Germany) to silanized samples was realized by using the homo-bifunctional BS^3 crosslinker (Thermo Fisher Scientific, Waltham, USA). For this purpose, 0.25 mM of this water-soluble crosslinker reagent was used to react with the primary amines of the previously silanized specimens at 4°C for 1 h in borate buffered saline (BBS, pH 8.5) under constant agitation. Silanized samples harboring connected BS^3 were gently washed with precooled BBS. Subsequently, the discs were immersed in the appropriate protein solution (1 µg/mL in BBS) for 2 h at 4°C with frequent shaking in order to enable covalently bonded proteins on the individual surfaces. In order to remove unbound proteins, the samples were washed three times with precooled BBS.

2.4 | Testing of mechanical exposure, acid and temperature resistance on modified surfaces

Natural teeth as well as dental implants are exposed to temperature fluctuations, different pH values, and mechanical stress. All surfaces in the oral cavity are surrounded by a protective layer, the pellicle, an acellular protein film of saliva-like origin that strongly adheres to the enamel of the tooth. Because of this fact, the modified test specimens were additionally conditioned with three different surface pretreatments in the following experiments: (1) untreated test specimens without contact with natural saliva (control), (2) test specimens exposed to sterile filtered saliva, and (3) test specimens with a pellicle layer formed in vitro, by exposing them for 1 min to the saliva of a healthy donor.

2.4.1 | Mechanical stability testing using a toothbrushing machine

The resistance of the modified surfaces to mechanical influences was tested using a toothbrushing machine (Figure S1). This was intended to simulate daily oral hygiene. The toothbrushing machine was manufactured in the scientific workshop of the University Hospital of RWTH Aachen University, Germany. The machine consisted of two reservoirs in which the specimens were fixed and clamped by means of a rail. A motor drive enabled the toothbrush heads to exert a linear movement. Weights of 100 g simulated the force exerted. A toothbrushing cycle lasting 30 min was performed with a toothpaste-slurry mixture in a ratio of 3:1 according to ISO 11609:2010 [28]. Afterwards, the samples were cleaned three different ways to remove remaining toothpaste-slurry: with ddH_2O, with ddH_2O in an ultrasonic bath, or with 70% ethanol in an ultrasonic bath. Subsequently, the samples were analyzed by AFM, SEM, and XPS to determine possible abrasion of the modified surface.

2.4.2 | Acid resistance testing

To assess the acid resistance, the samples were alternately exposed to an acidic environment of pH = 5 and a neutral environment of pH = 7 for 30 min each. For this purpose, a demineralization solution was prepared according to Tschoppe et al. and a remineralization solution according to Buskes et al.[28,29] The composition of the demineralization and remineralization solutions used is listed in Table 1. Subsequently, the modified surfaces were evaluated as described above.

2.4.3 | Analysis of temperature stability

In order to simulate temperature extremes a thermocycler (SD Mechatronik, Feldkirchen-Westerham, Germany) was used. For this purpose, the samples were alternately transferred to reservoirs at 5 and 55°C with a total of 1600 cycles. The samples were held in the corresponding reservoirs for 5 s each. Subsequently, the samples were analyzed via SEM, AFM, and XPS.

TABLE 1 Composition of the demineralization and remineralization solution.

Type of solution	Chemicals
Demineralization solution Tschoppe et al.[28]	2.2 mM $CaCl_2 \times H_2O$, 2.2 mM KH_2PO_4, 0.0476 mM NaF, 50 mM CH_3COOH, and 10 mM KOH, add ddH_2O, adjust pH value to 5.0
Remineralization solution Buskes et al.[29]	1.5 mM $CaCl_2 \times H_2O$, 0.9 mM KH_2PO_4, 1 M 4-2-hydroxy-ethyl-1-piperazineethanesulfonic acid(HEPES) buffer, add ddH_2O, adjust pH value to 7.0

2.5 | Ninhydrin assay

In order to detect the density of the amines within the APDS before and after mechanical, temperature, and acid exposure, a ninhydrin assay was performed. To accomplish this, the individual specimens were treated with ninhydrin reagent (Merck, #1.06705.0100, Darmstadt, Germany) and were incubated overnight protected from light.

2.6 | Surface characterization

2.6.1 | X-ray photoelectron spectroscopy

XPS measurements were carried out using an Ultra Axis spectrometer (Kratos, Manchester, UK) equipped with monoenergetic AlKα1,2 (1486.7 eV, 144 W) radiation in order to assess elemental surface composition and to verify the presence of APDS on Y-TZP substrates.

2.6.2 | Atomic force microscopy

The NanoStation II (SiS, Germany) was used in the tapping mode to locate the APDS profile on sapphire (Y:ZrO2-YSZ; CrysTec, Berlin, Germany) after treatment with the toothbrushing machine. The PPP-NCLR cantilever (NANOSENSORS, Neuchatel, Switzerland) was placed randomly on the individual samples, and three images with magnifications of 20 × 20 µm, 5 × 5 µm, and 3.5 × 3.5 µm were recorded. All AFM images were analyzed using NanoScope 9.1 software (Bruker, Billercia, USA) to observe the respective surface topographies.

2.6.3 | Scanning electron microscopy

The samples, previously dried at room temperature, were analyzed in a SEM (Environmental scanning electron microscope FEI

Quattro S, Thermo Fisher Scientific, FEI, Netherlands). Here, it is of importance that the samples were not sputtered with a layer of gold–palladium in order to avoid the appearance of artifacts on the surface.

2.7 | Fluorescence labeling of the ECM protein

In order to confirm the presence of applied human fibronectin on Y-TZP discs after 21 days at 37°C in phosphate-buffered saline (PBS), immunofluorescence microscopy was performed. The remaining proteins on the surface were fixed with 4% (w/v) paraformaldehyde(PFA) for 10 min and blocked with bovine serum albumin (BSA, Sigma Aldrich, St. Louis, USA) for 1 h at room temperature. Next, the specimens were incubated overnight at 4°C with the primary antibody anti-fibronectin (1:200 dilution, #MAB1918, mouse monoclonal, R&D Systems, Minneapolis, USA). The remaining antibody solution was removed by 5-min wash steps with PBS, and afterwards samples were incubated with Alexa Fluor 488 (1:2000 dilution, #A21121, goat anti-mouse, Invitrogen, Waltham, USA) for 1 h at room temperature. Finally, bound antibodies were detected using fluorescence microscopy (Axio Imager 2, Carl Zeiss, Oberkochen, Germany).

2.8 | Isolation of human gingival fibroblasts

Human gingival tissue was obtained with written informed consent (EK 266/19) as required by the ethics committee of the Faculty of Medicine of RWTH Aachen University, Aachen, Germany from clinically healthy donors undergoing routine surgical interventions. For the collection of human gingival fibroblasts (HGFs), the gingiva tissue was mechanically separated into epithelial and connective tissue during surgical procedures. The obtained tissue was disinfected in 70% ethanol and washed in PBS solution (Gibco, Waltham, USA) containing 1% (v/v) penicillin–streptomycin. The connective tissue was cut into small pieces, and the explants were placed into 25 cm^2 culture flasks. After the explants had 30 min to adhere to the bottom of the culture flask, they were carefully covered with 3 mL of culture medium (Dulbecco's modified Eagle's medium, DMEM, high glucose, Sigma Aldrich, St. Louis, USA) supplemented with 10% (v/v) fetal calf serum (FCS, PAN Biotech, Aidenbach, Germany), 2% (v/v) L-glutamine (Sigma Aldrich, St. Louis, USA), and 1% (v/v) penicillin–streptomycin (Thermo Fisher Scientific, Waltham, USA). The 25 cm^2 culture flasks were placed in a moisturized incubator at a temperature of 37°C and an atmosphere with 5% CO_2. Cells were subcultured at 80% confluency with 0.05% trypsin/0.02% ethylenediaminetetraacetic acid (EDTA, PAN Biotech, Aidenbach, Germany) solution.

2.9 | Live/dead staining of HGFs

HGFs were seeded at a density of 1×10^5 cells/mL on the different surface conditions. After 1 and 3 days of cultivation at 37°C and 5% CO_2, HGFs were stained with fluorescein diacetate (FDA) and propidium iodide (PI) in order to distinguish between live and dead cells. To accomplish this, 10 µL of FDA and PI were combined in 600 µL Ringer's solution. Immediately afterwards, 20 µL of the staining solution was transferred on the samples with the cells on top. Finally, the stained HGFs were visualized using a fluorescence microscope (Axio Imager 2, Carl Zeiss, Oberkochen, Germany).

2.10 | Detection of fibronectin using western blot

In order to identify proteolytic stability of the crosslinked fibronectin, the samples were incubated with trypsin (PAN Biotech, Aidenbach, Germany), collagenase from *Clostridium histolyticum* (Worthington Biochemical Corporation, Lakewood, USA) and saliva. For this purpose, the enzymes and saliva were incubated for 30 min, 2 h, and 6 h on the samples. Afterwards, 15 µL of collected supernatant of each condition was mixed with 4× Laemmli sample buffer (Bio-Rad Laboratories Inc., USA) containing the reducing agent β-mercaptoethanol (Sigma Aldrich, St. Louis, USA). The samples were then transferred into the pockets of the 4%–20% Criterion TGX Stain-Free Protein Gel (18 well, 30 µL, Bio-Rad Laboratories Inc., Hercules, USA), which was inserted in a gel electrophoresis chamber filled with Running Buffer (Tris/Tricine/sodium dodecyl sulfate(SDS)-Running Buffer, Bio-Rad Laboratories Inc., USA). Proteins were separated by their size at 40 mA for 15 min increasing to 80 mA for additional 20 min.

For the blotting process, the anode stack was inserted on the bottom of the Trans-Blot Turbo Transfer System device (Bio-Rad Laboratories Inc., Hercules, USA) and the SDS gel was placed bubble free on the polyvinylidene fluoride(PVDF) membrane. The gel was additionally covered with a water-soaked filter paper and finally with the cathode stack. The blotting procedure took 7 min, according to the programmed parameters. After the protein transfer was complete, the membrane was blocked for 10 min with EveryBlot Blocking Buffer (Bio-Rad Laboratories Inc., Hercules, USA) on an orbital shaker (neoLab, Heidelberg, Germany). The primary antibody solution (anti-fibronectin, diluted 1:1000, #MAB1918, R&D Systems, Minneapolis, USA) was then diluted in 3% BSA in PBS supplemented with 1% Tween and was incubated overnight at 4°C under continuous agitation. The remaining antibody solution was removed by three 15 min wash steps using PBS containing 1% Tween (TPBS, Sigma Aldrich, St. Louis, USA), and the membrane was then incubated for 1 h with the secondary antibody conjugated with horseradish peroxidase (goat anti-mouse IgG (H+L)-HRP conjugate, diluted 1:50000, #1706516, Bio-Rad Laboratories Inc., Hercules, USA) also diluted in 3% BSA in TPBS. Afterwards, the membrane was washed three times as described above. Finally, bound antibodies were detected by chemiluminescence after adding luminol (Cytiva Amersham ECL Select Western Blotting Detection Reagent, Chicago, USA). After incubation for 3 min, the bands on the PVDF membrane were visualized using the LAS-3000 Imager (Fujifilm, Minato, Japan).

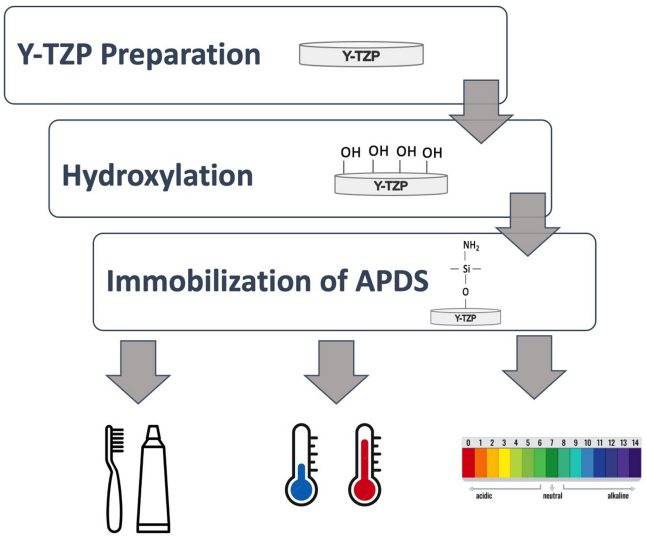

SCHEME 1 Workflow of the individual modification steps of the Y-TZP samples and the subsequent testing against mechanical, thermal, and acidic influences. APDS, 3-aminopropyldiisopropylethoxysilane.

2.11 | Statistical and image analysis

For characterization of the surface conditions, AFM, XPS, and SEM were performed at least three random spots on the specimens. The cell culture experiments were repeated in three independent experiments with at least three different HGF donors. Cells were visualized with a fluorescence microscope (Axio Imager 2; Carl Zeiss, Oberkochen, Germany) using 10× objective. Images were recorded at room temperature, and randomly selected areas of the samples were captured.

3 | RESULTS

In this study, we investigated the influence of acid, temperature, and mechanical stress on the APDS-modified surfaces. For this purpose, the Y-TZP samples were prepared and treated with piranha solution (mixture of sulfuric acid and hydrogen peroxide) to increase the hydroxyl groups on the surface. The hydroxyl groups were then used as attachment points for the APDS. The modified construct was then tested against the above mentioned effects (Scheme 1).

3.1 | Surface characterization after mechanical exposure

The topography of the APDS-functionalized surface of Y-TZP sapphires after treatment with the toothbrushing machine was investigated using AFM (Figure 1). In Figure 1A larger particles on the surface can be observed. Since the Sa value appeared to be quite high at 6.77 ± 0.06 nm, the surface was additionally examined at a higher magnification. Remarkably, the Sa value decreased to 0.70 ± 0.71 nm at a higher magnification of 5 × 5 µm (Figure 1B). In addition, an area without the presence of particles was analyzed, marked with a black frame in Figure 1B. Here, a Sa value of 0.09 ± 0.01 nm was obtained (Figure 1C).

The chemical composition analyzed via XPS after mechanical exposure and different cleaning strategies is shown in Table 2. The coupled silane was detected on all Y-TZP specimens after treatment with the toothbrushing machine and subsequent cleaning. However, from Table 2 it can be deduced that most of the silane remained on Y-TZP specimens that were cleaned with ddH_2O only. The element zinc is a part of the toothpaste mixture and was also detected during the measurement. The XPS spectra of the samples treated with the toothbrushing machine with the respective cleaning strategies can be seen in Figure S2A-D.

Furthermore, the surface was examined by SEM (Figure 2A–N). The analysis revealed that no differences were detectable between native and APDS-modified specimens with regard to surface texture after mechanical treatment. The surfaces were additionally covered with sterile filtered and pure saliva. No dissimilarities between these conditions could be observed. It is worth mentioning that in the lower row the stripes of the slurry were clearly visible.

3.2 | Surface characterization after acid and temperature treatment

The AFM images of APDS-modified sapphires after acid and thermal treatment are shown in Figure 3. The acid treated samples revealed a Sa value of 0.48 ± 0.16 nm and relatively smooth surface structure (Figure 3A), whereas specimens exposed to different temperatures revealed a much higher rougher Sa value (6.36 ± 1.81 nm, Figure 3B).

XPS analysis showed that silicon was detected on both thermal and acid treated samples (Table 3). It is noticeable that there was more silicon on the acid treated samples in contrast to the samples treated with the thermocycler. In addition, a nitrogen content of 9.67% was measured on the thermocycler treated samples. An increased carbon proportion (63.07%) was also visible for thermal treated specimens. XPS survey of the thermal and acid treated specimens is shown in Figure S3A,B.

In Figure 4 it can be seen that there is no difference between the Y-TZP-APDS-modified and native samples after acid treatments in terms of surface quality. Furthermore, no difference was visualized between the sterile saliva-coated and saliva-coated specimens.

This observation was also recorded in the thermal-treated samples (Figure 5). However, more impurities can be observed on the surface of the APDS-coated samples.

Furthermore, a ninhydrin assay was performed after all treatment and cleaning strategies in order to detect any remaining amino groups. Figure 6 showed that on all APDS-coated samples, the —NH_2 groups were still present. However, a reduced density of amino groups was observed on thermal treated samples.

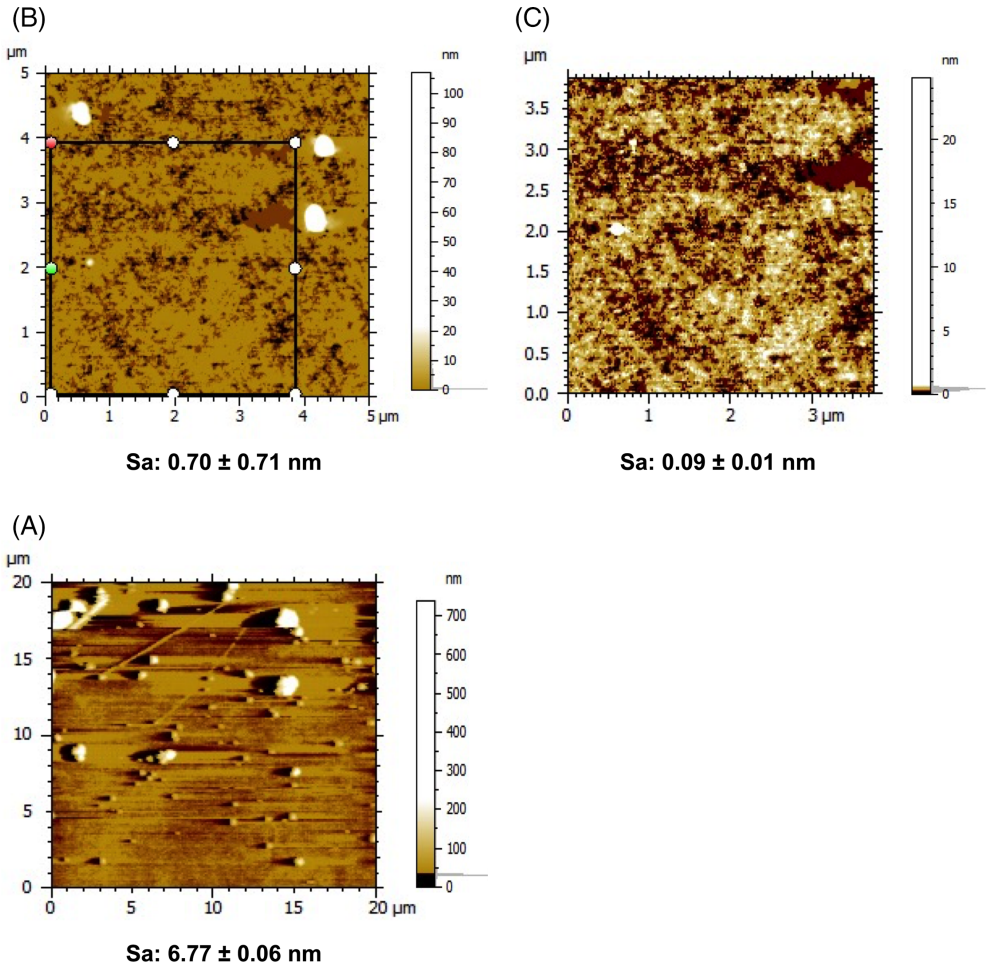

FIGURE 1 3-Aminopropyldiisopropylethoxysilane-coated Y-TZP sapphires treated with a toothbrushing machine. The atomic force microscopy image in (A) has a magnification of 20 × 20 µm, in (B) 5 × 5 µm, and in (C) approximately 3.5 × 3.5 µm.

TABLE 2 Chemical composition (in atomic %) of silanized Y-TZP samples after mechanical treatment and different cleaning strategies.

	O 1s	C 1s	Zr 3d	Zn 2p	Si 2p
Y-TZP (native)	58.03	15.53	24.90	-	-
Y-TZP + APDS (ultrasonic bath with 70% ethanol)	52.25	25.70	16.19	4.11	1.74
Y-TZP + APDS (ddH_2O)	47.48	33.70	15.20	1.45	2.18
Y-TZP + APDS (ultrasonic bath with ddH_2O)	46.85	32.87	15.20	2.19	1.98

Note: The native specimen was used as a control.
Abbreviation: ADPS, 3-aminopropyldiisopropylethoxysilane.

3.3 | Gingival fibroblast activity on treated surfaces

The gingival fibroblasts in each group showed the typical spindle morphology and similar growth trends (Figure 7). Interestingly, specimens cleaned with ethanol after treatment with the toothbrushing machine (ToBrMa) revealed the lowest growth behavior at day one. Furthermore, Y-TZP samples modified with APDS exhibited slightly higher cell growth ability. After 3 days of culture, the cells covered almost the entire surface of the Y-TZP specimens (Figure 7).

3.4 | Stability of crosslinked fibronectin

The stability of fibronectin crosslinked to the silanized zirconia surface was analyzed for enzymatic degradation. The fibronectin possibly detached by the enzymes was then detected by western blot. Figure 8 revealed that neither treatment with collagenase and trypsin nor application of saliva resulted in visualization of detached fibronectin at any time of analysis. A clear signal of fibronectin is detectable only in the positive control (Figure 8).

In addition, the hydrolysis stability of the crosslinked fibronectin stored for 21 days in PBS was investigated by immunofluorescence.

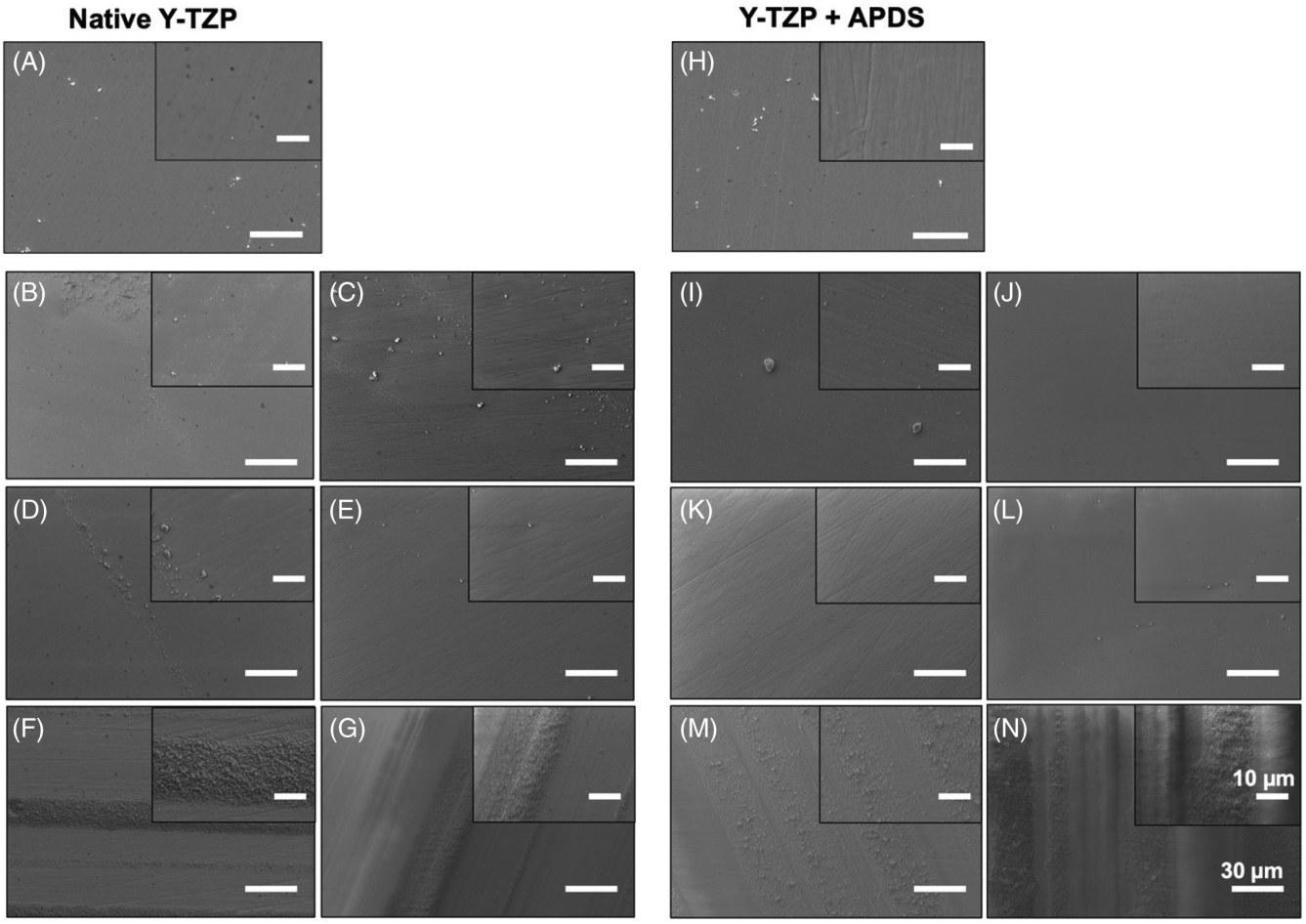

FIGURE 2 Scanning electron microscopy images of native and 3-aminopropyldiisopropylethoxysilane (APDS)-modified Y-TZP specimens after treatment using a toothbrushing machine and individual cleaning mechanisms. (A) Native Y-TZP (control), (B) native Y-TZP coated with saliva and cleaned with ddH_2O, (C) native Y-TZP coated with sterile filtered saliva and cleaned with ddH_2O, (D) native Y-TZP coated with saliva and cleaned with ddH_2O in ultrasonic bath, (E): native Y-TZP coated with sterile filtered saliva and cleaned with ddH_2O in ultrasonic bath, (F) native Y-TZP coated with saliva and cleaned with ethanol in ultrasonic bath, (G) native Y-TZP coated with sterile filtered saliva and cleaned with ethanol in ultrasonic bath, (H) APDS-modified Y-TZP (control), (I) APDS treated Y-TZP cleaned with ddH_2O, (J) APDS treated Y-TZP coated with sterile filtered saliva and cleaned with ddH_2O, (K) APDS treated Y-TZP coated with saliva and cleaned with ddH_2O in ultrasonic bath, (L) APDS treated Y-TZP coated with sterile filtered saliva and cleaned with ddH_2O in ultrasonic bath, (M) APDS treated Y-TZP coated with saliva and cleaned with ethanol in ultrasonic bath, (N) APDS treated Y-TZP coated with sterile filtered saliva and cleaned with ethanol in ultrasonic bath. Scale bars in micrograph overviews: 30 µm; scale bars in magnifications (corners on top right of each micrograph overview): 10 µm.

FIGURE 3 Topography of 3-aminopropyldiisopropylethoxysilane (APDS)-functionalized Y-TZP sapphires after acid and temperature exposure. Atomic force microscopy images show (A) acid treated sapphires and (B) specimens, which were alternatingly soaked in water reservoirs of 5 and 55°C. Magnification of images: 5 × 5 µm.

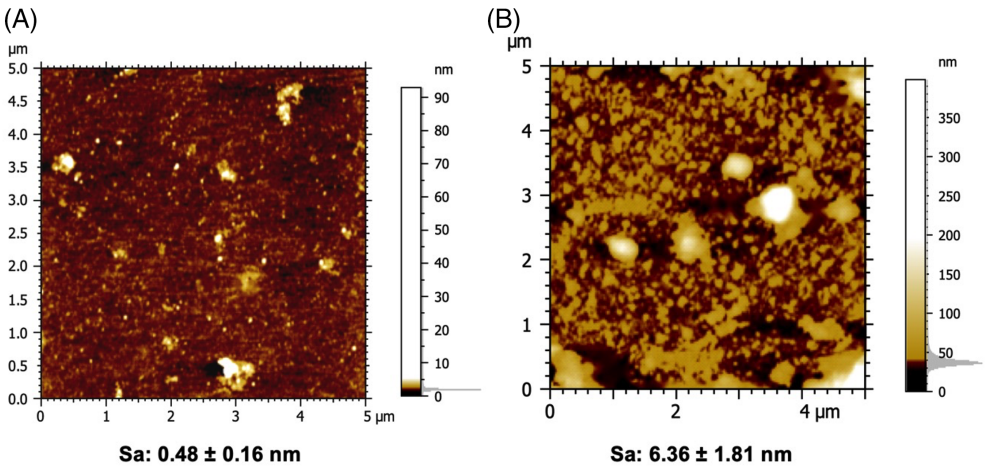

	O 1s	N 1s	C 1s	Zr 3d	Y 3d	Si 2p
Y-TZP + APDS (acid treated)	53.86	-	27.38	14.78	0.99	2.89
Y-TZP + APDS (thermal treated)	24.25	9.67	63.07	0.82	-	2.20

Abbreviation: ADPS, 3-aminopropyldiisopropylethoxysilane.

TABLE 3 Chemical composition (in atomic %) of APDS-modified Y-TZP samples after temperature and acid treatment.

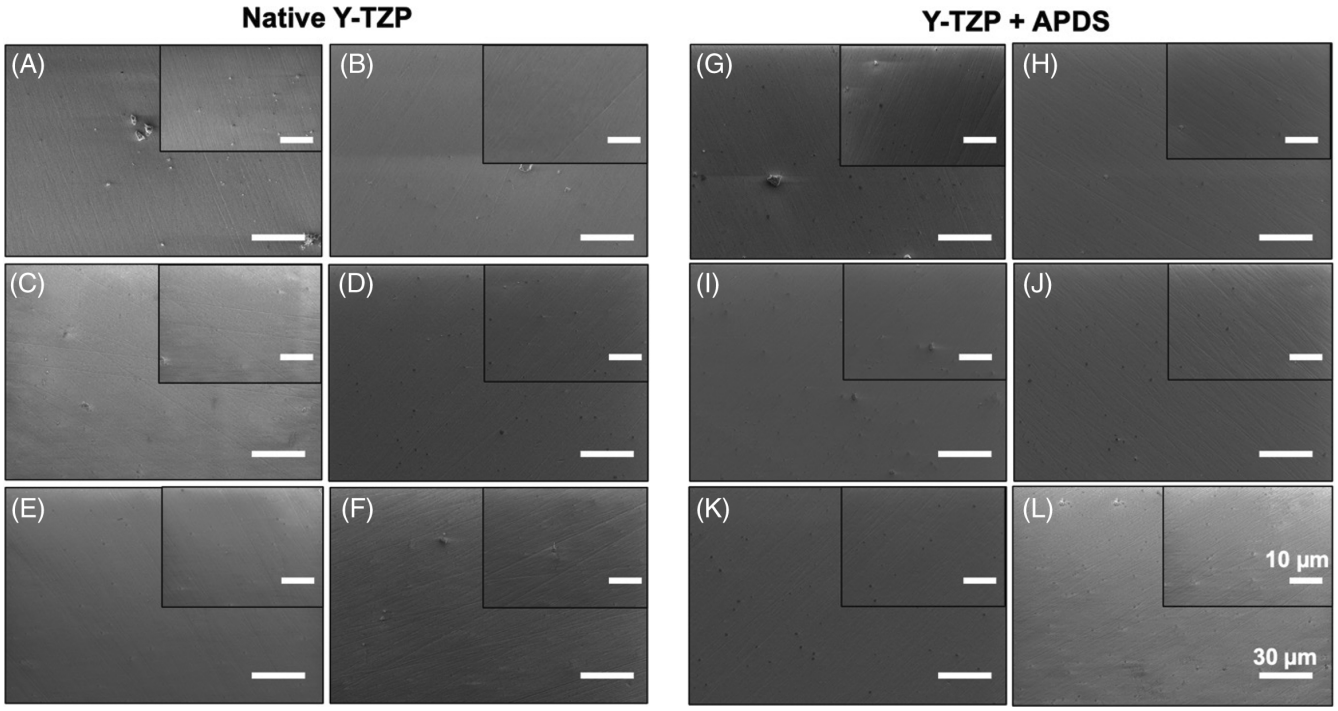

FIGURE 4 Scanning electron microscopy images of native and 3-aminopropyldiisopropylethoxysilane (APDS)-modified specimens after acid treatment. (A) Native Y-TZP without acid treatment (control), (B) native Y-TZP with acid treatment, (C) native Y-TZP without acid treatment and sterile filtered saliva, (D) native Y-TZP with acid treatment and sterile filtered saliva, (E) native Y-TZP without acid treatment and saliva, (F) native Y-TZP with acid treatment and saliva, (G) APDS-modified Y-TZP without acid treatment (control), (H) APDS-modified Y-TZP with acid treatment, (I) APDS-modified Y-TZP without acid treatment and sterile filtered saliva, (J) APDS-modified Y-TZP with acid treatment and sterile filtered saliva, (K) APDS-modified Y-TZP without acid treatment and saliva, and (L) APDS-modified Y-TZP with acid treatment and saliva. Scale bars in micrograph overviews: 30 µm; scale bars in magnifications (corners on top right of each micrograph overview): 10 µm.

The fluorescence image showed that a clear signal from the remaining attached fibronectin could be confirmed even after 21 days of incubation in the aqueous environment (Figure 9).

4 | DISCUSSION

Because of the structural differences between the peri-implant soft tissue and the soft tissue around natural teeth, external stimuli can more easily penetrate the peri-implant barrier and influence the implant abutment surface. Effective and, above all, durable functionalization of dental implant abutments can optimize the attachment of the soft tissue to the abutment surface. Such functionalization of the abutment surface should be able to withstand temperature and pH fluctuations, and mechanical influences in the oral cavity. In our previous study, we were able to show that the functionalization of abutment materials using silane can facilitate the adhesion of HGFs. Therefore, the aim of this study was to investigate the stability of APDS-modified Y-TZP against these mentioned influences. Because silane molecules can also interact with other biomolecules, fibronectin was coupled via a crosslinker to the surface. Here the hydrolytic stability and degradation resistance were analyzed. Daily toothbrushing is essential to the reduction or prevention of the development of plaque and peri-implant diseases. In particular, prevention of plaque (biofilm) formation around the abutment is essential for the maintenance of the soft-tissue barrier.[30] One objective of this study was to test how mechanically induced abrasion generated by a toothbrushing machine affects our surface modification (abrasiveness). Various methods for testing abrasiveness using a toothbrushing machine have been described in the literature.[28,31–33] De Almeida et al. tested the abrasiveness on surfaces of various dental restorations, including silane-treated ceramics, using a toothbrushing machine.[30] Here, 150 g of mass was mounted on the toothbrush head and a total of 10,000–14,600 toothbrushing cycles were performed.[30] In the study by De Almeida et al., the samples were subsequently analyzed by SEM. Their results showed that the surface roughness was higher after treatment

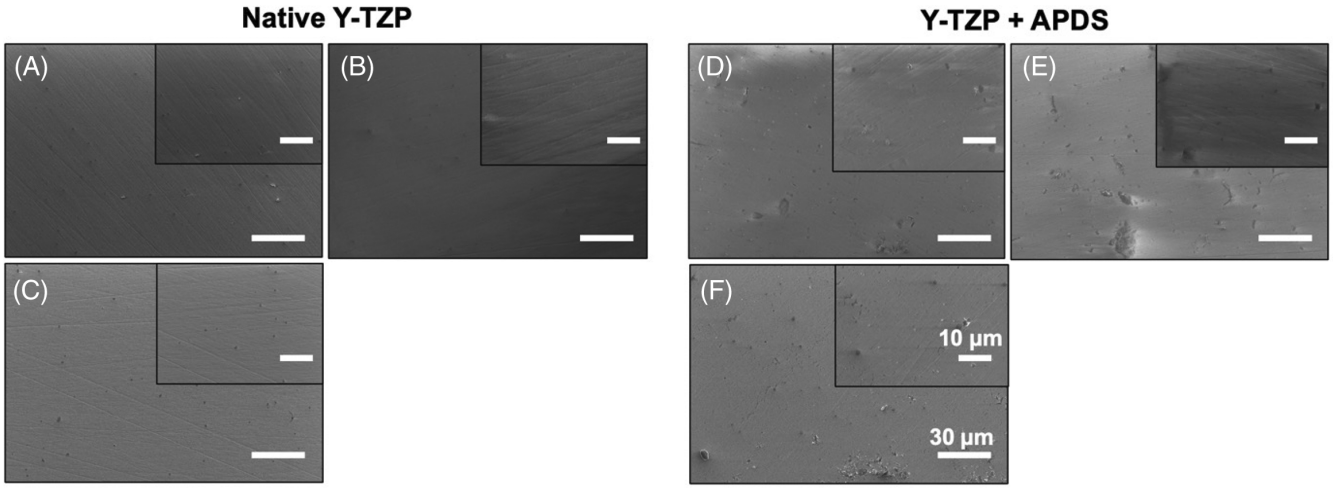

FIGURE 5 Scanning electron microscopy images of native and 3-aminopropyldiisopropylethoxysilane (APDS)-modified specimens after thermocycler treatment. (A) Native Y-TZP (control), (B) native Y-TZP with sterile filtered saliva, (C) native Y-TZP with saliva, (D) Y-TZP functionalized with APDS (control), (E) APDS-modified Y-TZP with sterile filtered saliva, and (F) APDS-modified Y-TZP with saliva. Scale bars in micrograph overviews: 30 µm, scale bars in magnifications (corners on top right of each micrograph overview): 10 µm.

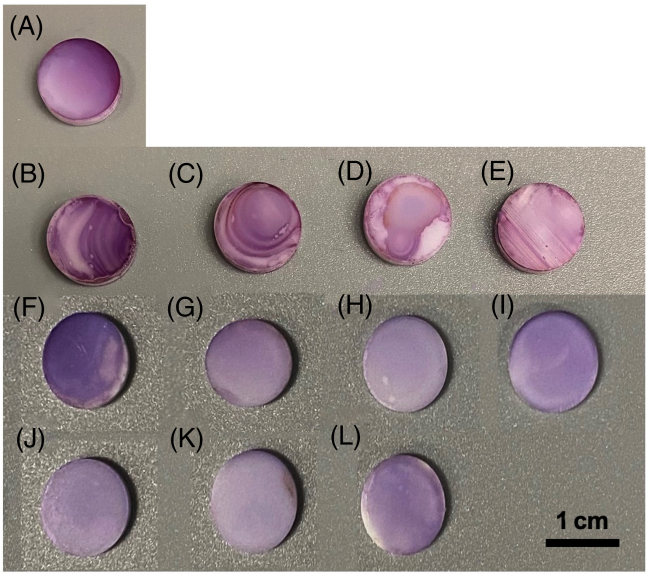

FIGURE 6 Ninhydrin assay of differently treated 3-aminopropyldiisopropylethoxysilane (APDS)-functionalized Y-TZP specimens. (A) APDS-modified Y-TZP (control), (B) APDS-treated Y-TZP coated with sterile filtered saliva and cleaned with ddH_2O, (C) APDS-treated Y-TZP coated with saliva and cleaned with ddH_2O, (D) APDS-treated Y-TZP coated with sterile filtered saliva and cleaned with ddH_2O in ultrasonic bath, (E) APDS-treated Y-TZP coated with saliva and cleaned with ddH_2O in ultrasonic bath, (F) APDS-treated Y-TZP coated with sterile filtered saliva and cleaned with ethanol in ultrasonic bath, (G) APDS-treated Y-TZP coated with saliva and cleaned with ethanol in ultrasonic bath, (H) APDS-modified Y-TZP with acid treatment, (I) APDS-modified Y-TZP with acid treatment and sterile filtered saliva, (J) APDS-modified Y-TZP with acid treatment and saliva, (K) APDS-modified Y-TZP with sterile filtered saliva treated with thermocycler, and (L) APDS-modified Y-TZP with saliva treated with thermocycler. Scale bar: 1 cm.

with the toothbrush simulator than before mechanical stress.[30] An increase in surface roughness was also detected by AFM in the present study (Figure 1). It is reasonable to assume that toothpaste residues were on the surface despite cleaning, which led to an increased roughness value. However, the AFM measurements at a high magnification of 3.5 × 3.5 µm showed areas on the specimens with a roughness value corresponding to that of the native specimens without mechanical stress.[34] Nevertheless, XPS analysis demonstrated that the silane layer was still present on the surface of Y-TZP specimens even after treatment with the toothbrushing machine and different cleaning strategies (Table 2).

In this study, the different surface conditions were also alternately incubated in the solutions with pH = 5 and pH = 7. AFM images (Figure 3A) revealed that the Sa value was near to that of untreated APDS-modified Y-TZP specimens.[34] Nevertheless, XPS analysis confirmed the presence of the silane monolayer (Table 3). In addition, the thermal stability of the different surface conditions was analyzed. For this purpose, the samples were alternately soaked in 5 and 55°C water reservoirs. Figure 3B showed rough surface after thermal treatment with a Sa value of 6.36 ± 1.81 nm. The atomic percentage of silicon measured via XPS showed a decrease compared with acid treated samples (Table 3). This might be a result of release of silane molecules from the surface due to the thermal process. The high roughness may possibly be due to the fact that the silane has come off in a few places and has partly taken on a different structure. Chandekar et al. compared the thermal stability of different silanes with different head groups.[35] The silanes deposited on silicon oxide, the 4-aminobutyltriethoxysilane SAMs were found to be indefinitely stable up to 250°C, while the 2H-perfluorodecyltriethoxysilane SAMs were stable up to 350°C. The thermal stabilities of silane SAMs compared with thiols were studied

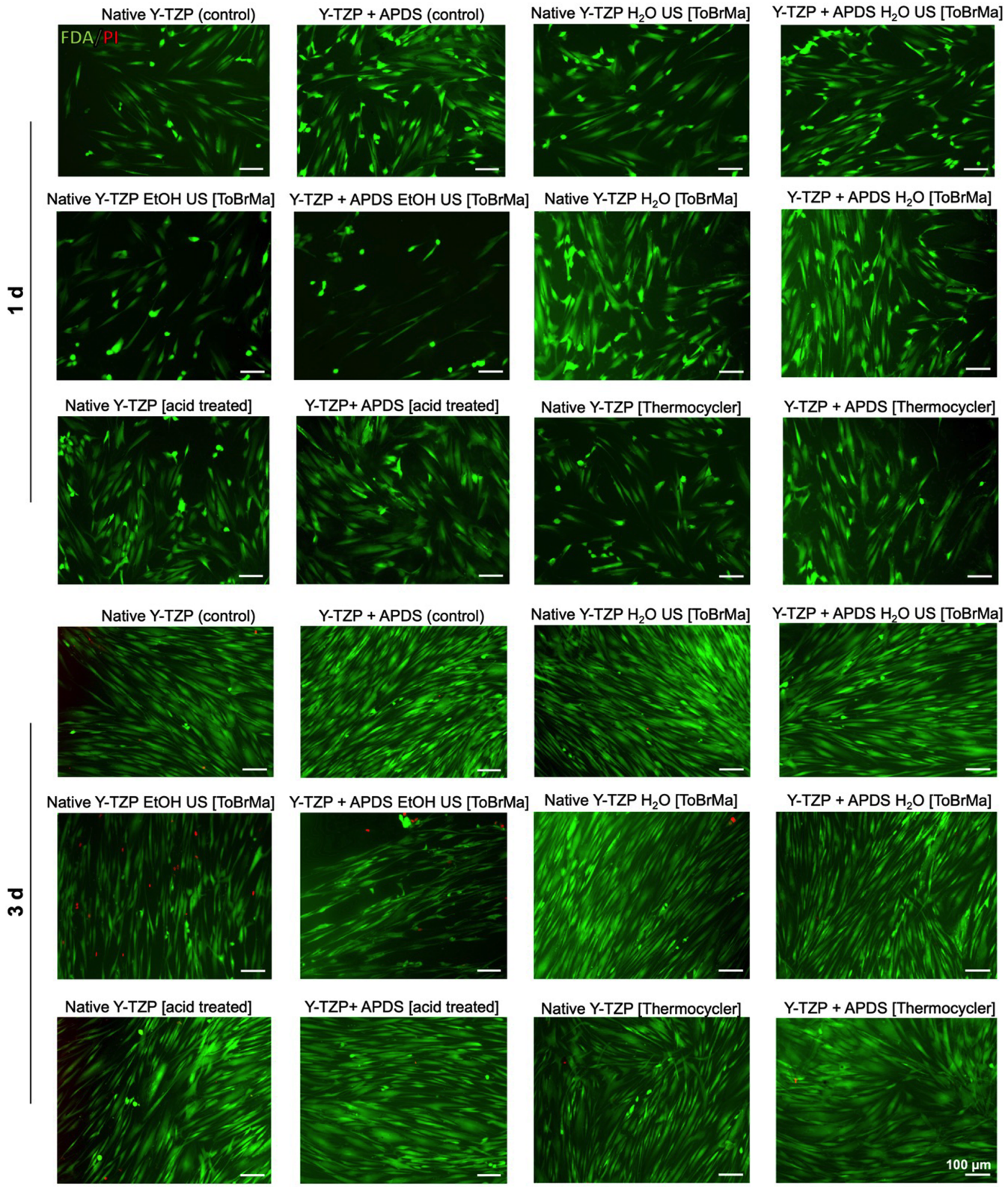

FIGURE 7 Live/dead staining of human gingival fibroblasts on differently treated Y-TZP specimens after 1 and 3 days. Living cells were stained with fluorescein diacetate, while dead cells appear red (stained with propidium iodide) under fluorescence microscope. Scale bars: 100 µm.

by Sagiv et al.[36] Because of their relatively weak S-metal bonds, thiol SAMs are likely to be less thermally stable than silane SAMs, in which the molecules are linked to each other and to the substrate by several strong covalent Si—O bonds. For each SAM type, the nature of the end group and the length of the tail have a significant effect on thermal stability. Furthermore, the type of tail group is expected

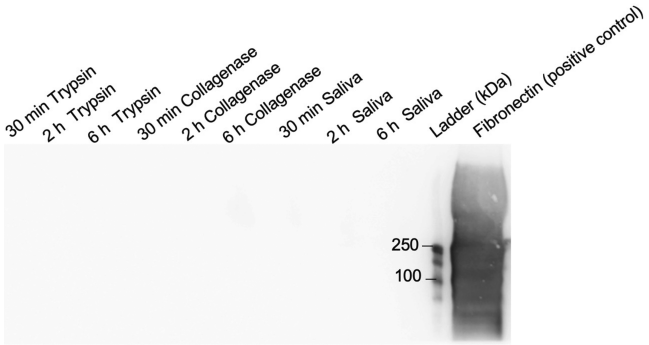

FIGURE 8 Stability against proteolytic degradation of crosslinked fibronectin assessed via western blot. Y-TZP samples crosslinked with fibronectin were incubated with trypsin, collagenase, or saliva at 37°C at different time points. The supernatant was analyzed by western blot.

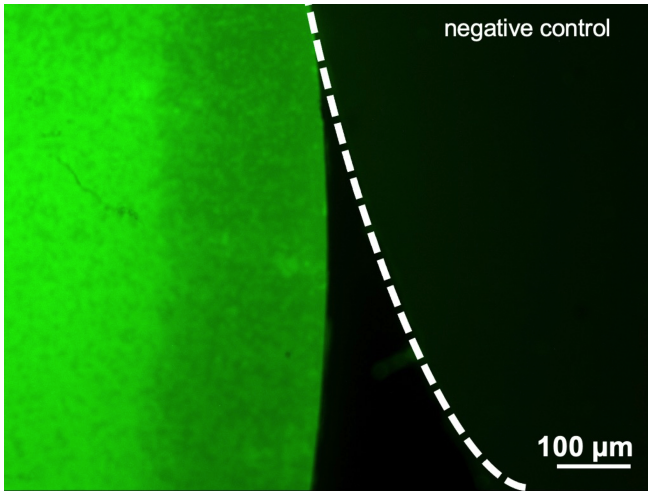

FIGURE 9 Hydrolysis stability of crosslinked fibronectin. The samples were stored for 21 days in phosphate-buffered saline at 37°C. Afterwards, the remaining fibronectin on the surface was visualized with Alexa Fluor 488. An unmodified specimen was used as a control (indicated through dashed line). Scale bar: 100 µm.

to have a significant effect on the degree of order and stability of the formed monolayers.

It has previously been described that fluorinated SAMs detach at 350°C from the surface but can withstand higher temperatures of up to 550°C under vacuum.[37] Bain et al. determined that alkanethiols desorbed at about 70°C, with the rate of desorption dependent on temperature, environment (air or type of contact liquid), and chain length.[38,39] In the tests performed, desorption was faster in a hydrocarbon solvent, slower in ethanol, and even slower in air. Using ellipsometric data, the authors also found that the longer the chain length, the more thermally stable the SAMs. Klein et al. examined the stability of SAMs based on nonfluorinated or fluorinated linear hydrocarbons by means of mechanical stress.[40] Mechanical friction on the smooth surfaces caused degradation of the molecules with amorphous and poorly defined monolayer with CH, CC, and CF bonds.[40]

For this reason, the function of NH_2-terminating SAMs was tested in this study in cell experiments after mechanical, thermal, and acid exposure. The live/dead staining revealed that fibroblasts showed similar growth trends on all surface conditions. After 3 days of incubation, the surface was almost covered by the cells (Figure 7). It can be assumed that the APDS remained stable after the treatment strategies applied within this study.

In contrast, Huser et al. used 3-(ethoxydimethylsilyl)propylamine (APDES) in their study in which the formation of silanols was observed regardless of the pH, which can be attributed to the catalytic effect of the amine group on the hydrolysis of the ethoxy groups.[41] However, the molar amount of silanols formed was lower at a basic pH than at an acidic pH. Furthermore, the grafting of APDES onto stainless steel was analyzed by XPS. Here, a distinct covalent bond between APDES and the stainless steel surface was detected, resulting in a uniform layer of adsorbed molecules. Moreover, this grafted layer is very stable as no removal of the alkoxysilane was observed after immersion in hot water, a property that is highly critical for these molecules.

It is worth mentioning that no SEM images of the different surface conditions showed any differences between sterile filtered and pure saliva coating (Figures 2, 4, and 5). The ninhydrin assay revealed that even with the incubation of the samples in sterile filtered and pure saliva, amino groups were still present after mechanical, thermal, and acid treatment (Figure 6). The exact mechanism of whether and how saliva protects the samples from external influences should be further investigated.

While many organic monolayers hydrolyze rapidly or after prolonged immersion (30 days), alkyne-based (Si—C bonded) monolayers on Si and, in particular, alkyne-based (C—O—C bonded) monolayers on SiC show excellent hydrolytic stability, even under extreme pH conditions and under physiological conditions (PBS buffer).[42]

In this study, we were able to show that the silane with the immobilized fibronectin remained stable over 21 days of hydrolysis even without a silicate layer (Figure 9). Based on enzymatic attacks in vivo, the entire modification construct on the Y-TZP samples was tested against enzymatic degradation in vitro (Figure 8). Here, the immobilized fibronectin on silanized samples appeared to be resistant to degradation, at least over a period of 6 h. Enzymes contained in saliva also showed no effect.

5 | CONCLUSION

It was confirmed that the formation of the APDS layer was stable even after mechanical exposure, and thermal, and acid treatment. Differences in saliva-coated and uncoated surfaces regarding protecting of the underlying APDS layer could not be observed. The HGFs covered the differently treated surfaces within 3 days and almost no dead cells could be detected. Furthermore, crosslinked fibronectin to silanized surfaces was hydrolytically stable for up to 21 days and revealed degradation resistance using different enzymes. Thus, we can conclude that the proposed functionalization method holds great

potential to withstand harmful effects within the oral cavity and remains unchanged on the surface.

ACKNOWLEDGMENTS

The authors would like to acknowledge the financial support from German Research Foundation (DFG) (grants FI 975/30-2 and WO 1576/6-2). In addition, the environmental scanning electron microscope FEI Quattro S was funded by the DFG –495328185. Furthermore, the authors thank Dr.rer.nat. Anke Aretz, Central Facility for Electron Microscopy, GFE, Aachen, Germany for conducting AFM analyses of the samples. Open Access funding enabled and organized by Projekt DEAL.

CONFLICT OF INTEREST STATEMENT

The authors declare no conflicts of interest.

DATA AVAILABILITY STATEMENT

The data that support the findings of this study are available from the corresponding authors upon reasonable request.

ORCID

Horst Fischer https://orcid.org/0000-0003-0990-5028

REFERENCES

1. López-Píriz R, Goyos-Ball L, Cabal B, et al. New ceramic multi-unit dental abutments with an antimicrobial glassy coating. *Materials*. 2022;15:5422.
2. Bechir F, Pacurar M, Tohati A, Bataga SM. Comparative study of salivary pH, buffer capacity, and flow in patients with and without gastroesophageal reflux disease. *Int J Environ Res Public Health*. 2021; 19:201.
3. Tanabe M, Takahashi T, Shimoyama K, Toyoshima Y, Ueno T. Effects of rehydration and food consumption on salivary flow, pH and buffering capacity in young adult volunteers during ergometer exercise. *J Int Soc Sports Nutr*. 2013;10:49.
4. Sang T, Ye Z, Fischer NG, et al. Physical-chemical interactions between dental materials surface, salivary pellicle and *Streptococcus gordonii*. *Colloids Surf B Biointerfaces*. 2020;190:110938.
5. Chawhuaveang DD, Yu OY, Yin IX, Lam WY-H, Mei ML, Chu C-H. Acquired salivary pellicle and oral diseases: a literature review. *J Dent Sci*. 2021;16:523-529.
6. Siqueira WL, Zhang W, Helmerhorst EJ, Gygi SP, Oppenheim FG. Identification of protein components in in vivo human acquired enamel pellicle using LC−ESI−MS/MS. *J Proteome Res*. 2007;6:2152-2160.
7. Hannig M. Ultrastructural investigation of pellicle morphogenesis at two different intraoral sites during a 24-h period. *Clin Oral Investig*. 1999;3:88-95.
8. Zhang F, Cheng Z, Ding C, Li J. Functional biomedical materials derived from proteins in the acquired salivary pellicle. *J Mater Chem B*. 2021;9:6507-6520.
9. Hannig M, Döbert A, Stigler R, Müller U, Prokhorova SA. Initial salivary pellicle formation on solid substrates studied by AFM. *J Nanosci Nanotechnol*. 2004;4:532-538.
10. Yao Y, Lamkin MS, Oppenheim E. Pellicle precursor proteins: acidic proline-rich proteins, statherin, and histatins, and their crosslinking reaction by oral transglutaminase. *J Dent Res*. 1999;78:1696-1703.
11. Fábián TK, Hermann P, Beck A, Fejérdy P, Fábián G. Salivary defense proteins: their network and role in innate and acquired oral immunity. *Int J Mol Sci*. 2012;13:4295-4320.
12. Buzalaf MAR, Hannas AR, Kato MT. Saliva and dental erosion. *J Appl Oral Sci*. 2012;20:493-502.
13. Kitagawa T, Tanimoto Y, Iida T, Murakami H. Effects of material and coefficient of friction on taper joint dental implants. *J Prosthodont Res*. 2020;64:359-367.
14. Golieskardi M, Satgunam M, Ragurajan D. Mechanical and microstructural evaluation of Y-TZP using microwave sintering technique. *Key Eng Mater*. 2016;706:36-41.
15. Wang J, Yin W, He X, Wang Q, Guo M, Chen S. Good biocompatibility and sintering properties of zirconia nanoparticles synthesized via vapor-phase hydrolysis. *Sci Rep*. 2016;6:35020.
16. Tchinda A, Chézeau L, Pierson G, Kouitat-Njiwa R, Rihn BH, Bravetti P. Biocompatibility of ZrO2 vs. Y-TZP alloys: influence of their composition and surface topography. *Materials*. 2022;15:4655.
17. Herráez-Galindo C, Rizo-Gorrita M, Maza-Solano S, Serrera-Figallo M-A, Torres-Lagares D. A review on CAD/CAM yttria-stabilized tetragonal zirconia polycrystal (Y-TZP) and polymethyl methacrylate (PMMA) and their biological behavior. *Polymers*. 2022; 14:906.
18. Koch FP. Zirkonoxid als dentales Implantatmaterial. *Der Freie Zahnarzt*. 2018;62:70.
19. Wu L, Eberhart M, Shan B, et al. Stable molecular surface modification of nanostructured, mesoporous metal oxide photoanodes by silane and click chemistry. *ACS Appl Mater Interfaces*. 2019;11:4560-4567.
20. Bhushan B. Self-assembled monolayers (SAMs) for controlling adhesion, friction, and wear. In: Bhushan B, ed. *Springer Handbook Nanotechnology*. Springer; 2007. Available from http://link.springer.com/10.1007/978-3-540-29857-1_43 [cited 2023 Mar 18].
21. Hasan A, Saxena V, Pandey LM. Surface functionalization of Ti6Al4V via self-assembled monolayers for improved protein adsorption and fibroblast adhesion. *Langmuir*. 2018;34:3494-3506.
22. Arima Y, Iwata H. Effects of surface functional groups on protein adsorption and subsequent cell adhesion using self-assembled monolayers. *J Mater Chem*. 2007;17:4079.
23. Schickle K, Korsten A, Weber M, Bergmann C, Neuss S, Fischer H. Towards osseointegration of bioinert ceramics: can biological agents be immobilized on alumina substrates using self-assembled monolayer technique? *J Eur Ceram Soc*. 2013;33:2705-2713.
24. Shuturminska K, O'Malley C, Collis DWP, Conde J, Azevedo HS. Displaying biofunctionality on materials through templated self-assembly. *Self-assembling Biomaterials*. Elsevier; 2018. Available from https://linkinghub.elsevier.com/retrieve/pii/B9780081020159000186 [cited 2023 Mar 18].
25. Pankov R, Yamada KM. Fibronectin at a glance. *J Cell Sci*. 2002;115: 3861-3863.
26. Chen X, Sevilla P, Aparicio C. Surface biofunctionalization by covalent co-immobilization of oligopeptides. *Colloids Surf B Biointerfaces*. 2013; 107:189-197.
27. Belsom A, Rappsilber J. Anatomy of a crosslinker. *Curr Opin Chem Biol*. 2021;60:39-46.
28. Tschoppe P, Zandim DL, Sampaio JEC, Kielbassa AM. Saliva substitute in combination with high-concentrated fluoride toothpaste: effects on demineralised dentin in vitro. *J Dent*. 2010;38:207-213.
29. Buskes JAKM, Christoffersen J, Arends J. Lesion formation and lesion remineralization in enamel under constant composition conditions. *Caries Res*. 1985;19:490-496.
30. De Almeida JRM, Messias AM, Gadelha DF, Caldas SGFR, Caldas MRGR. Evaluation of surface characteristics and weight variation of different composite resins after simulated toothbrushing. *Eur J Gen Dent*. 2020;9:141-146.
31. AlAli M, Silikas N, Satterthwaite J. The effects of toothbrush Wear on the surface roughness and gloss of resin composites with various types of matrices. *Dent J*. 2021;9:8.
32. Garcia FCP, Wang L, D'Alpino PHP, de Souza JB, de Araújo PA, de Lia Mondelli RF. Evaluation of the roughness and mass loss of the

flowable composites after simulated toothbrushing abrasion. *Braz Oral Res*. 2004;18:156-161.
33. Bizhang M, Schmidt I, Chun Y-HP, Arnold WH, Zimmer S. Toothbrush abrasivity in a long-term simulation on human dentin depends on brushing mode and bristle arrangement. *PLoS One*. 2017;12: e0172060.
34. Palkowitz AL, Tuna T, Bishti S, et al. Biofunctionalization of dental abutment surfaces by crosslinked ECM proteins strongly enhances adhesion and proliferation of gingival fibroblasts. *Adv Healthc Mater*. 2021;10:2100132.
35. Chandekar A, Sengupta SK, Whitten JE. Thermal stability of thiol and silane monolayers: a comparative study. *Appl Surf Sci*. 2010;256: 2742-2749.
36. Sagiv J. Organized monolayers by adsorption. 1. Formation and structure of oleophobic mixed monolayers on solid surfaces. *J Am Chem Soc*. 1980;102:92-98.
37. Prakash P, Satheesh U, Devaprakasam D. Photocatalytic and thermolytic "attenuation–degradation" mechanisms of perfluoroalkylsilane self assembled on TiO_2 nanoparticles. *Appl Surf Sci*. 2021;549:149278.
38. Bain CD, Troughton EB, Tao YT, Evall J, Whitesides GM, Nuzzo RG. Formation of monolayer films by the spontaneous assembly of organic thiols from solution onto gold. *J Am Chem Soc*. 1989;111: 321-335.
39. Srisombat L, Jamison AC, Lee TR. Stability: a key issue for self-assembled monolayers on gold as thin-film coatings and nanoparticle protectants. *Colloids Surf A Physicochem Eng Asp*. 2011;390: 1-19.
40. Klein RJ, Fischer DA, Lenhart JL. Thermal and mechanical aging of self-assembled monolayers as studied by near edge x-ray absorption fine structure. *Langmuir*. 2011;27:12423-12433.
41. Huser J, Bistac S, Delaite C, Dentel D, Derivaz M, Zanouni M. Hydrolysis and grafting of dimethylalkoxysilanes onto stainless steel: grafting of alkoxysilanes onto stainless steel. *Surf Interface Anal*. 2015;47: 523-528.
42. Bhairamadgi NS, Pujari SP, Trovela FG, et al. Hydrolytic and thermal stability of organic monolayers on various inorganic substrates. *Langmuir*. 2014;30:5829-5839.

SUPPORTING INFORMATION

Additional supporting information can be found online in the Supporting Information section at the end of this article.

How to cite this article: Palkowitz AL, Tuna T, Kaufmann R, Buhl EM, Wolfart S, Fischer H. Functionalization of a zirconia surface by covalently immobilized fibronectin and its effects on resistance to thermal, acid, and mechanical exposure. *J Biomed Mater Res*. 2024;112(2):e35390. doi:10.1002/jbm.b.35390